

Extended Stern Model

Rangadhar Pradhan*, Analava Mitra and Soumen Das

School of Medical Science and Technology, Indian Institute of Technology Kharagpur, West Bengal, India

Abstract: In this paper, a theoretical approach of extended Stern model is formulated to represent the electric double layer for biochemical as well as biological samples. The existing Stern model is used for several decades to describe the phenomena of electric double layer of electrode/electrolyte interface. In the conventional Stern model the double layer which is formed between the electrode and electrolyte interface is described by double layer capacitance. Using the existing Stern model, the equivalent circuit model is not valid for electrical double layer capacitance of electrode/electrolyte interface in β dispersion range for biologically relevant samples. The protein molecules form chemical coupling and chemical adsorption along with classical ionic bonding with gold electrodes. Thus, the compactness of electric double layer decreases and the double layer capacitance is replaced by a constant phase element. In the present paper, a three-electrode based electric cell-substrate impedance sensing device was used to measure the impedance of various enzymatic solutions for validation of theoretical approach. The results obtained from experimental work, were simulated by equivalent circuit simulator, ZsimpWin to validate the extended Stern model by comparing χ^2 value. Finally the electrical parameters were extracted and compared for Stern model and extended Stern model. The results obtained by practical experiment and equivalent circuit simulation showed the effectiveness of extended Stern model over the existing Stern model.

Keywords: Stern model, Electric double layer, double layer capacitance, constant phase element, enzymatic solutions.

1. INTRODUCTION

The understanding of electrode/electrolyte interface phenomena has great importance in electrochemistry, electrokinetics, microfluidics, bioimpedance, and electric cell-substrate impedance sensing (ECIS). When a metal electrode is immersed into an electrolytic solution, an electric double layer (EDL) is formed at interface between metal and electrolyte. This double layer plays a crucial role in electrode/electrolyte interfacial phenomena. Stern model is used for several decades to describe the EDL [1-3]. Several advances have been made to understand the influence of EDL on physical and chemical systems. In the lower frequency range up to 1 kHz the polarization effect takes place at the electrode and electrolytic interface. Thus in α dispersion range, the double layer capacitance is replaced by constant phase element (CPE). However polarization effect is absent in higher frequency range, but several authors replaced double layer capacitance by CPE in both cases of enzymatic solution and live tissue and cell experiments [4-7]. However the mechanism of enzymatic phenomena happening at electrode surface and thus modified the double layer capacitance has not been properly investigated in β dispersion range of frequency. The present paper will discuss the theoretical phenomena of EDL and development of extended Stern model which is suited

for biochemical solution over the gold electrode surface. Finally the present hypothesis has been experimentally validated by using microelectrode based ECIS device and different enzymes in PBS solution.

2. THEORY

2.1. Stern Model

When a metal electrode is immersed into an electrolytic solution, an EDL is formed at interface between metal and electrolyte. One layer of charge is located at the metal surface and the other, of equal and opposite charge, just inside the electrolytic solution. Stern developed the double layer theory to describe EDL by taking the finite size of the counterions and their binding properties at the surface into account [8]. The diffuse layer is divided into two layers such as inner Stern layer followed by outer Gouy-Chapman layer as shown in Figure 1.

The impedance of electrode/electrolyte interface arises from the charge transfer within the Stern layer and the impedance of the Gouy-Chapman layer [9]. The resistive elements are Nernst impedance controlled by the charge transfer (R_{CT}) and Warburg impedance (Z_W) controlled by the diffusion process within the Gouy-Chapman layer. The electrical double layer behaves like a lossy capacitor (C_S) due to limited charge mobility within it and the electrolytes behave as resistor (R_S) [10]. Thus the equivalent circuit model for electrode-electrolyte system comprises Warburg impedance in series with charge transfer resistance

*Address corresponding to this author at the School of Medical Science and Technology, Indian Institute of Technology Kharagpur, West Bengal, 721302, India; Tel: +913222281228; Fax: +913222282221; E-mail: rangadhar@iitkgp.ac.in

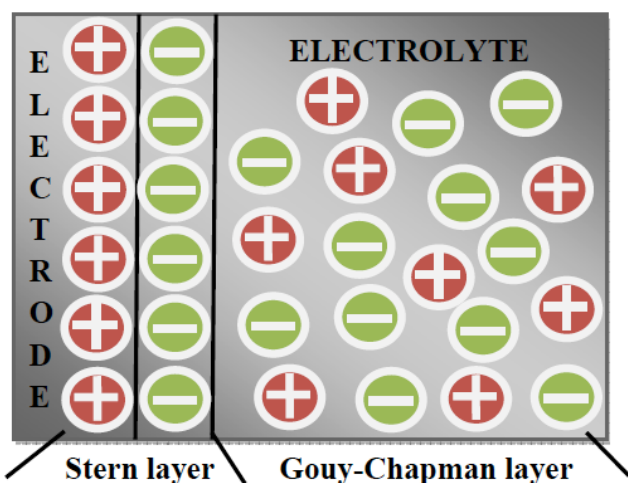


Figure 1: Schematic of Stern Model at electrode/electrolyte interface.

(R_{CT}) shunted by double layer capacitance(C_s), together in series with bulk resistance (R_s) as shown in Figure 2. This model along with its equivalent circuit suits well for measuring electrode/electrolyte interface impedance [11]. Several authors introduced constant phase element (CPE) instead of double layer capacitance to describe the polarization effect in low frequency up to 1 kHz. However in higher frequencies this model works suitably for electrolytic solution as polarization effect is absent [12-13]. But this model does not work properly for most of the biochemical as well as biological molecules [6]. Thus, a new extended Stern model is being proposed to describe the interface impedance of biochemical as well as biological samples.

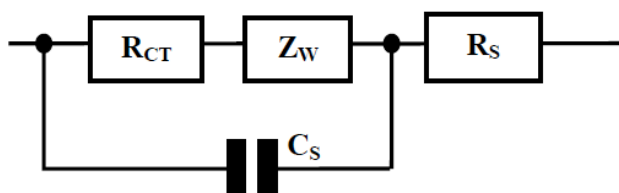


Figure 2: Equivalent circuit of electrode/electrolyte interface.

2.2. Extended Stern Model

In general gold metal is used as the electrode for ECIS study because it is inert and does not react with the electrolytes as compared to other metal like aluminum. However gold has inherent property to bind covalently with protein molecules having alkanethiols, cysteines, cysteamines and disulphides groups. Also sulphides, thioethers, thiocarbamates, nitriles, and cyanides groups are coupled with gold by chemical adsorption (CA) process [14]. Thus when these groups are present in biochemical or biomolecular solution, the

electric double layer formation is being distorted. By considering this hypothesis a new model has been proposed as depicted in Figure 3.

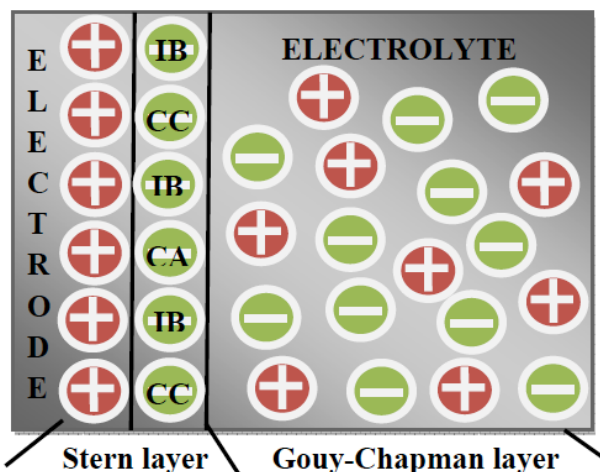


Figure 3: Extended Stern model.

As the covalent coupling (CC) is the strongest bonding, the covalent groups replace some of the ionic groups within ionic bonding (IB) available in electrolytic solution. Although chemical adsorption controlled by Van der Waals bonding is the weakest bond than others, it forms lesser amount of bonding within electrode surface. So along with ionic bonds, covalent bonds and Van der Waals bonds are found in the same EDL, which influence the formation of double layer capacitance. Thus both ionic and covalent coupling forms inhomogeneous bonding on the surface. As a result the compactness of double layer capacitance decreases as the covalent coupling increases resulting replacement of double layer capacitance by a constant phase element. The impedance of CPE, $Z(\omega)$ is expressed as,

$$Z(\omega) = \frac{1}{Q} (j\omega)^n \quad (1)$$

Where, $j = \sqrt{-1}$, $0 < n < 1$ and Q is a constant with dimension Fs^{n-1} .

The equivalent circuit model comprises Warburg impedance in series with charge transfer resistance (R_{CT}) shunted by CPE (Q_{dl}), together in series with bulk resistance (R_s) as shown in Figure 4.

3. MATERIALS AND METHODS

3.1. Device Fabrication

The three electrodes e.g. working electrode (WE), reference electrode (RE), and counter electrode (CE)

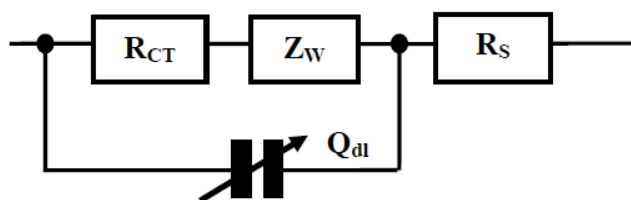


Figure 4: Modified Equivalent circuit for enzymatic solution.

of a ECIS device configuration was adopted for the present experimental study. The dimensions of WE, RE, and CE are defined as $200 \times 200 \mu\text{m}$, $2000 \times 2000 \mu\text{m}$, and $2000 \times 2000 \mu\text{m}$ respectively. The device was fabricated on 2 inch diameter Pyrex wafers using metal deposition and photolithography techniques. Initially, the wafers were cleaned and a thin layer of chromium (Cr) and gold (Au) were thermally evaporated onto the wafers. Subsequently, the electrode traces and its contact pads were lithographically defined using positive photoresist and then the Cr and Au layers were selectively removed by wet etching process to define the metal patterns on the substrate. Finally, a second lithography step was performed to apply another photosensitive polymer (SU8) layer as passivation coating over the metal electrodes. In this step, only the electrode sensors and contact pads were exposed to make contact with the electrolyte as shown in Figure 5. The photoresist was hard baked to impart stability and inertness to the polymer. The wafers were then diced into single devices for subsequent packaging and measurements. Finally the individual device was fixed in a printed circuit board and electrical connections were taken from device to external equipment using thin metal wires and then cloning cylinders were aligned and attached to serve as electrolyte reservoir around the three electrode system by using PDMS as glue.

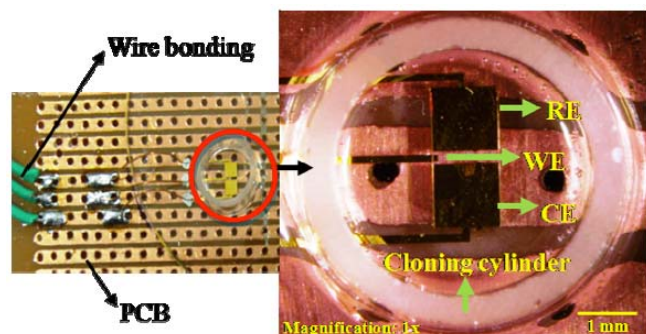


Figure 5: Microphotograph of a three-electrode device.

3.2. Enzyme Solution Preparation

Five different types of enzymes such as human fibroblast collagenase, glucose oxidase (GOD) from

Aspergillus niger, lysozyme from egg white, human pepsin, and horse radish peroxidase (HRP) were taken for the present study. One percent solution of enzyme in PBS has been used as the biochemical sample to perform the impedance measurement.

3.3. Impedance Measurement

The electrical impedance measurement of different enzyme solutions was carried out using computer controlled electrochemical work station SP 150 (Bio-Logic, France) by connecting the fabricated device directly to the system. All the measurements were performed with actuation voltage of 10mv and frequency range from 100Hz to 1 MHz with 51 sample points in between in a logarithmic scale. All the measurements were repeated for ten times and then averaged to get the impedance value for each frequency. The present electrochemical workstation has an inbuilt facility to reduce the noise margin of the measured impedance data through software interpretation. The Nyquist data was obtained from the devices of four designs and subsequently exported to ZsimpWin software for further analysis for equivalent circuit simulation.

3.4. Equivalent Circuit Simulation

The impedance data found from practical experimentation was imported to ZsimpWin (Version 3.10) to validate the real world experiment. The modeling was performed by iterative process by considering an equivalent circuit that resembles the electrode/electrolyte environment. In this process chi-square (χ^2) value for the entire model plays a significant role to validate the simulation results. Also the electrochemical theories and the Boukamp suggestion help to choose the components in such a way, that addition of each component should reduce χ^2 value by one-order of magnitude [15]. The χ^2 value of the order of $1.5\text{E}-3$ or below was acceptable for a given model [16].

4. RESULTS AND DISCUSSIONS

Figure 6 represents the Bode plot of different enzymes measured by fabricated microelectrode based ECIS devices along with the equivalent circuit. It is observed from the Figure 6 that with increase of frequency the impedance value decreases steadily up to 100 kHz and then it saturates for all the enzymes. The phase angle decreases up to 1 kHz and then increases up to 1 MHz. However the Warburg

impedance is absent in the experimental data set due to use of 100Hz to 1 MHz frequency range and gold microelectrodes [17-19]. Thus the measured impedance data of electrolytic solution of different enzymes were then simulated to ZSimpWin software to validate the impedance data by using equivalent circuit model of Stern model as well as the Extended Stern model without Warburg impedance. The extracted values of electrical equivalent parameters with relative standard error (e %) of different enzymes along with the χ^2 values are listed in Table 1.

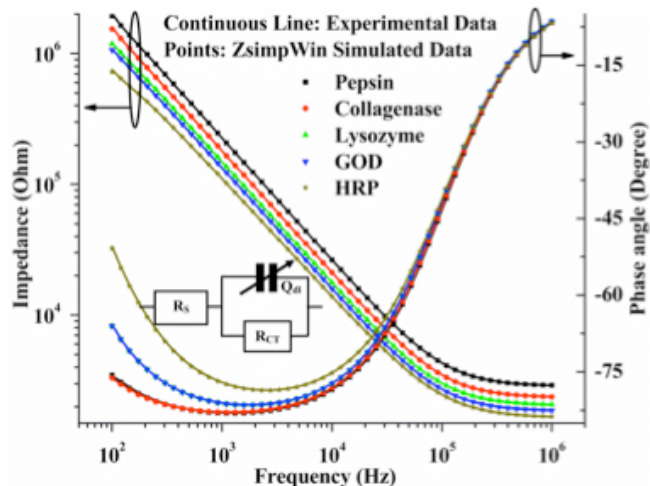


Figure 6: Bode plot of various enzymes with the equivalent circuit.

From the above table it is evident that the χ^2 value is at least 3 orders less for equivalent circuit using CPE model as compared to Stern model for all the different enzymatic solutions. Also the percentage of error is

more in case of equivalent circuit describing Stern model. This result validates the extended Stern model in which the double layer capacitance is replaced by CPE in the electrical double layer between electrode and electrolyte interface throughout the frequency range. This result is attributed due to the presence of disulphide groups and cysteines in all the enzymes [20-24] that forms covalent coupling replacing ionic bonding with the gold electrodes surface. Moreover minute chemical adsorption also takes place on the electrode surface due to presence of various adsorbing groups. Thus along with ionic bonds, covalent bonds and Van der Waals bonds are also present in EDL which helps to replace double layer capacitance by constant phase element.

5. CONCLUSIONS

In this paper a theoretical approach of Extended Stern model is formulated for electrode/electrolyte interface. In the existing Stern model electrical double layer behaves like a capacitor due to limited charge mobility within it and the electrolytes behaves as resistor. In case of extended Stern model, the modified double layer capacitance is replaced by constant phase element to represent covalent coupling as well as chemical adsorption taking place at the electrode surface for any biological systems. Also the experimental realization of this assumption of Extended Stern model showed expected result obtained from equivalent circuit simulation. However several more experiments are needed to study the surface chemistry of electrode/electrolyte interface for biochemical and

Table 1: Electrical Equivalent Parameters of the Impedance Data for Various Enzymes with Relative Standard Error (e %)

Parameters	Pepsin		Collagenase		Lysozyme		GOD		HRP	
	Data	e %	Data	e %	Data	e %	Data	e %	Data	e %
Stern Model [R(CR) Equivalent Circuit]										
$R_s (\Omega)$	3080	3.15	2523	3.24	2218	3.41	2001	4.93	1831	4.09
$C_{s}(Fs^{-n-1})$	6.4E-10	1.97	8E-10	2.04	9E-10	2.20	1.07E-9	3.13	1.24E-9	2.75
$R_{CT}(\Omega)$	6.06E6	17.01	4.90E6	17.75	2.42E6	12.01	1.30E17	9.26E11	9.92E5	9.19
χ^2 value	1.41E-2		1.51E-2		1.71E-2		3.56E-2		2.50E-2	
Extended Stern Model [R(QR) Equivalent Circuit]										
$R_s (\Omega)$	2868	0.21	2342	0.15	2045	0.08	1840	0.09	1643	0.19
$Q_{dl} (Fs^{-n-1})$	1.15E-9	0.52	1.4E-9	0.36	1.8E-9	0.20	2.09E-9	0.21	2.94E-9	0.48
n_{dl}	0.94	0.05	0.94	0.03	0.93	0.02	0.93	0.02	0.91	0.05
$R_{CT} (\Omega)$	1.21E7	2.67	1.05E7	2.01	3.80E6	0.51	3.42E6	0.52	1.37E6	0.64
χ^2 value	5.32E-5		2.55E-5		7.80E-6		7.81E-6		3.97E-5	

biological samples to strengthen the concept of Extended Stern Model.

ACKNOWLEDGEMENT

The authors thank the staff members of the MEMS Lab, IIT Kharagpur for their support towards this work.

REFERENCES

- [1] Bard AJ, Larry R. Faulkner *Electrochemical Methods: Fundamentals and Applications*. 2nd ed. New York: John Wiley & Sons 2000.
- [2] Hunter RJ. *Foundations of colloid science*. 2nd ed. New York: Oxford University 2001.
- [3] Grimnes S, Martinsen ØG. *Bioimpedance and Bioelectricity Basics*. 2nd ed. London: Academic Press 2000.
- [4] Ding S-J, Chang B-W, Wu C-C, Lai M-F, Chang H-C. Electrochemical evaluation of avidin–biotin interaction on self-assembled gold electrodes. *Electrochim Acta* 2005; 50: 3660-6. <http://dx.doi.org/10.1016/j.electacta.2005.01.011>
- [5] Dulay S, Lozano-Sánchez P, Iwuoha E, Katakis I, O'Sullivan CK. Electrochemical detection of celiac disease-related anti-tissue transglutaminase antibodies using thiol based surface chemistry. *Biosens Bioelectron* 2011; 26: 3852-6. <http://dx.doi.org/10.1016/j.bios.2011.02.045>
- [6] Moulton SE, Barisci JN, Bath A, Stella R, Wallace GG. Studies of double layer capacitance and electron transfer at a gold electrode exposed to protein solutions. *Electrochim Acta* 2004; 49: 4223-30. <http://dx.doi.org/10.1016/j.electacta.2004.03.034>
- [7] Huang H, Ran P, Liu Z. Impedance sensing of allergen–antibody interaction on glassy carbon electrode modified by gold electrodeposition 2007; 70: 257-62.
- [8] Stern O. Zur Theorie der Elektrolytischen Doppelschicht. *Z Elektrochem* 1924; 30: 508-16.
- [9] Franks W, Schenker I, Schmutz P, Hierlemann A. Impedance characterization and modeling of electrodes for biomedical applications. *IEEE Trans Biomed Eng* 2005; 52: 1295-302. <http://dx.doi.org/10.1109/TBME.2005.847523>
- [10] Pradhan R, Mitra A, Das S. Characterization of electrode/electrolyte interface for bioimpedance study. *Proceeding of IEEE Students' Technology Symposium (TechSym) 2011*; pp. 275-80.
- [11] Wang H, Varghese J, Pilon L. Simulation of electric double layer capacitors with mesoporous electrodes: Effects of morphology and electrolyte permittivity. *Electrochim Acta* 2011; 56: 6189-97. <http://dx.doi.org/10.1016/j.electacta.2011.03.140>
- [12] Sanabria H, Miller JH Jr. Relaxation processes due to the electrode-electrolyte interface in ionic solutions. *Phys Rev E Stat Nonlin Soft Matter Phys* 2006; 74: 051505. <http://dx.doi.org/10.1103/PhysRevE.74.051505>
- [13] Taylor DM, Macdonald AG. AC admittance of the metal/insulator/electrolyte interface. *J Phys D Appl Phys* 1987; 20: 1277. <http://dx.doi.org/10.1088/0022-3727/20/10/010>
- [14] Göpel W, Heiduschka P. Interface analysis in biosensor design. *Biosens Bioelectron* 1995; 10: 853-83. [http://dx.doi.org/10.1016/0956-5663\(95\)99225-A](http://dx.doi.org/10.1016/0956-5663(95)99225-A)
- [15] Boukamp BA. *Equivalent Circuits: Users Manual*. 2nd ed. Netherlands. University of Twente 1993.
- [16] Cui X, Martin DC. Electrochemical deposition and characterization of poly(3,4-ethylenedioxythiophene) on neural microelectrode arrays. *Sens Actuators B Chem* 2003; 89: 92-102. [http://dx.doi.org/10.1016/S0925-4005\(02\)00448-3](http://dx.doi.org/10.1016/S0925-4005(02)00448-3)
- [17] Richardot A, McAdams ET. Harmonic analysis of low-frequency bioelectrode behavior. *IEEE Trans Med Imaging* 2002; 21: 604-12. <http://dx.doi.org/10.1109/TMI.2002.800576>
- [18] McAdams ET, Jossinet J. Physical interpretation of Schwan's limit voltage of linearity. *Med Biol Eng Comput* 1994; 32: 126-30. <http://dx.doi.org/10.1007/BF02518908>
- [19] Franks W, Schenker I, Schmutz P, Hierlemann A. Impedance characterization and modeling of electrodes for biomedical applications. *IEEE Trans Biomed Eng* 2005; 52: 1295-302. <http://dx.doi.org/10.1109/TBME.2005.847523>
- [20] Nigel CV. Horseradish peroxidase: a modern view of a classic enzyme. *Phytochemistry* 2004; 65: 249-59. <http://dx.doi.org/10.1016/j.phytochem.2003.10.022>
- [21] Raba J, Mottola HA. Glucose Oxidase as an Analytical Reagent. *Crit Rev Anal Chem* 1995; 25: 1-42. <http://dx.doi.org/10.1080/10408349508050556>
- [22] Schwalbe H, Grimshaw SB, Spencer A, et al. A refined solution structure of hen lysozyme determined using residual dipolar coupling data. *Protein Sci* 2001; 10: 677-88. <http://dx.doi.org/10.1110/ps.43301>
- [23] Springman EB, Angleton EL, Birkedal-Hansen H, Van Wart HE. Multiple modes of activation of latent human fibroblast collagenase: evidence for the role of a Cys73 active-site zinc complex in latency and a "cysteine switch" mechanism for activation. *Proc Natl Acad Sci USA* 1990; 87: 364-8. <http://dx.doi.org/10.1073/pnas.87.1.364>
- [24] Fujinaga M, Chernaia MM, Mosimann SC, James MNG, Tarasova NI. Crystal structure of human pepsin and its complex with pepstatin. *Protein Sci* 1995; 4: 960-72. <http://dx.doi.org/10.1002/pro.5560040516>